Science of the Total Environment 512–513 (2015) 62–73

Contents lists available at ScienceDirect

Science of the Total Environment

journal homepage: www.elsevier.com/locate/scitotenv

Documentation of time-scales for onset of natural attenuation in an aquifer treated by a crude-oil recovery system

Violaine Ponsin [a,b], Joachim Maier [c], Yves Guelorget [c], Daniel Hunkeler [d], Daniel Bouchard [d], Hakeline Villavicencio [d], Patrick Höhener [a,*]

[a] Aix-Marseille Université-CNRS, Laboratoire Chimie Environnement FRE, 3416 Marseille, France
[b] French Environment and Energy Management Agency, 20 avenue de Grésillé, BP 90406 Angers Cedex 01, France
[c] ICF Environnement, 14/30 rue Alexandre Bâtiment C F, 92635 Gennevilliers, France
[d] Centre for Hydrogeology, University of Neuchâtel, Rue Emile-Argand 11, CH-2000 Neuchâtel, Switzerland

HIGHLIGHTS

- One of the world largest terrestrial oil spills is studied for 4 years.
- Initially pristine aerobic groundwater turns anoxic in 8 months.
- Sulfate reduction is the most important redox process thereafter.
- Biologically enhanced dissolution of toluene and benzene is evidenced.
- Stable carbon isotopes prove the degradation of benzene and ethylbenzene.

ARTICLE INFO

Article history:
Received 20 November 2014
Received in revised form 13 January 2015
Accepted 13 January 2015
Available online 21 January 2015

Editor: D. Barcelo

Keywords:
La Crau nature reserve
Benzene
Hydrocarbon spill
Aquifer
Biodegradation
Stable carbon isotopes

ABSTRACT

A pipeline transporting crude-oil broke in a nature reserve in 2009 and spilled 5100 m^3 of oil that partly reached the aquifer and formed progressively a floating oil lens. Groundwater monitoring started immediately after the spill and crude-oil recovery by dual pump-and-skim technology was operated after oil lens formation. This study aimed at documenting the implementation of redox-specific natural attenuation processes in the saturated zone and at assessing whether dissolved compounds were degraded. Seven targeted water sampling campaigns were done during four years in addition to a routine monitoring of hydrocarbon concentrations. Liquid oil reached the aquifer within 2.5 months, and anaerobic processes, from denitrification to reduction of sulfate, were observable after 8 months. Methanogenesis appeared on site after 28 months. Stable carbon isotope analyses after 16 months showed maximum shifts in $\delta^{13}C$ of $+4.9 \pm 0.22$‰ for toluene, $+2.4 \pm 0.19$‰ for benzene and $+0.9 \pm 0.51$‰ for ethylbenzene, suggesting anaerobic degradation of these compounds in the source zone. Estimations of fluxes of inorganic carbon produced by biodegradation revealed that, in average, 60% of inorganic carbon production was attributable to sulfate reduction. This percentage tended to decrease with time while the production of carbon attributable to methanogenesis was increasing. Within the investigation time frame, mass balance estimations showed that biodegradation is a more efficient process for control of dissolved concentrations compared to pumping and filtration on an activated charcoal filter.

1. Introduction

Most of petroleum hydrocarbon-contaminated sites in Europe are industrial sites or storage sites (Van Liedekerke et al., 2014). These sites are often subjected to progressive and slowly emerging contamination, created for example by leaking tanks, and once the pollution is discovered, it is difficult to assess when the groundwater ecosystem switched from a pristine system to a contaminated one because historical data are rarely available. A major industrial accident such as a pipeline rupture is different because the moment when the pollution occurs is generally clearly identified by a loss of pressure followed by discontinuation of delivery. The United States have more than 240,000 km of oil pipeline (Trench, 2003), and the average annual number of crude-oil pipeline spills per year per 1000 miles was 1.5 (i.e. 0.9 per 1000 km) for the 2007–2009 period, for a total amount of oil released of 111 m^3 (Delin and Herkelrath, 2014). In comparison, oil pipelines in Europe represent a total length of 36,000 km and the average annual number of pipeline oil spills (including crude oil and oil products) per 1000 km was 0.22 for the 2008–2012 period, for a total amount of 371 m^3 of oil released

* Corresponding author.
E-mail address: patrick.hohener@univ-amu.fr (P. Höhener).

http://dx.doi.org/10.1016/j.scitotenv.2015.01.033
0048-9697/

(Davis et al., 2013). These numbers suggest that the consequences of pipeline bursts on the environmental vulnerability of aquifers merits further research.

The crude-oil spill in Bemidji (Minnesota, USA) is a textbook case regarding pipeline spill research. A pipeline rupture in 1979 contaminated a shallow aquifer with 1700 m^3 of oil. The United States Geological Survey (USGS) Toxic Substances Hydrology Program sponsored a long-term and interdisciplinary project that started in 1983 (Delin et al., 1998). The objective of the project was to improve the understanding of the mobilization, transport, and fate of crude oil in the shallow subsurface. Work at the Bemidji site has ranged from characterization of microscopic-scale microbes-mineral interactions (Hiebert and Bennett, 1992; Bennett et al., 2000; Roberts, 2004; Rogers and Bennett, 2004) to plume-scale geochemical and microbial evolution (Baedecker et al., 1993; Bennett et al., 1993; Eganhouse et al., 1993; Cozzarelli et al., 1994; Bekins et al., 1999), and has included testing of complex models of multiphase flow, reactive transport, and biodegradation (Essaid et al., 1995, 2003; Curtis, 2003; Molins et al., 2010). More recent work focused on processes occurring in the vadose zone (Chaplin et al., 2002; Amos et al., 2005; Sihota and Mayer, 2012). One of their most important conclusions is that transport and fate of hydrocarbons in the subsurface is a spatially and temporally complex problem, and that only long-term monitoring can help to understand and predict the evolution of subsurface hydrocarbon plumes. Although work at Bemidji gave a very complete insight into processes occurring on the long-term at such a site, the very initial phases of the evolution of natural attenuation were not studied in great detail due to the absence of research programs in the initial years.

Very few studies actually described the early stages of aerobic and anaerobic degradation after a sudden pollution. Most of those studies were performed on dedicated sites deliberately contaminated to avoid problems associated with poorly defined sources and plumes. The mass of pollutants spilled at those sites are orders of magnitudes smaller compared to the masses at crude-oil pipeline bursts. Käss and Schwille (1992) poured about four m^3 of heating oil into the alluvial aquifer of the Rhine valley in order to study the formation of a hydrocarbon plume but they were not able to document complete geochemical reactions at the time of their pioneering work that started before 1980. The sandy Borden research aquifer in Ontario (Canada) was another such a site: secured distinct parts of this sandy aquifer were used for numerous studies on artificial pollutant release. Natural attenuation of coal tar creosote mixed with aquifer material to create a source zone was thoroughly studied in Borden (King et al., 1999; Fraser et al., 2008), and the first sampling campaign for monitoring of soluble compounds such as phenol, *m*-xylene and naphthalene was done 55 days after source emplacement (King and Barker, 1999). However, most of the processes that control the fate of hydrocarbons, such as aerobic degradation, were already occurring at Borden, and mass release and study duration were often not sufficient to document the change of redox state in this aquifer.

On August 7th, 2009, a pipeline transporting crude oil buried at 1 m depth broke in a steppe grassland nature reserve of restricted access, 50 km northwest of Marseille (France), and about 5100 m^3 of oil under pressure were projected to the surface where they spread across 5 ha of flat arid landscape. The crude oil later infiltrated through consolidated material via fractures, and formed a floating oil body in the underlying aquifer. The largest extension of the pool was covering about 4 ha. The underlying aquifer is the most important regional aquifer (520 km^2) and is under high pressure for water supply (Roux, 2006). It has been thus thoroughly studied since 1975 and a model was developed by the French Geological Survey to achieve optimal water management (Berard et al., 1995). In view of potential application of natural attenuation as management option at this site, research on the evolution of attenuation processes was initiated from the very beginning. Monitoring in La Crau started as soon as wells were drilled, while oil had not yet reached the aquifer and was still migrating through the vadose zone.

The objectives of this study were: (1) to monitor the temporal and spatial evolution of redox processes in the saturated zone during a four-year period following a massive oil spill in a pristine aquifer (2), to assess when and where hydrocarbon degradation and especially benzene degradation was occurring (3) to quantify ongoing biotic degradation processes through mass balances and carbon fluxes, and (4) to identify the dominant redox processes.

2. Material and methods

2.1. Site description

The site is in the "La Crau" alluvial plain, on 16 m above sea level (Fig. 1). This plain was formed by the former river Durance during the Pleistocene (Naudet et al., 2004). Deposits are made of coarse gravel of various alpine rocks with fine gravel and sand in the interstices. They are cemented in the upper meters by calcareous concretions formed by evaporation, in the form of a Puddingstone with fractures (Figure S1, Sup. mat). The deeper parts of the gravel deposits are free from concretions, have hydraulic conductivities of $0.2–2 * 10^{-3}$ m s^{-1}, and form the most important regional aquifer used for irrigation and drinking water supply. Gravel deposits extend over approximately 15 m and overlay silt or sandy-silt deposits of low permeability. The groundwater table is at 8–11 m below surface and shows important seasonal variations of up to 3 m caused by local rainfall and irrigation upgradient. The groundwater quality is well documented, and concentrations of aqueous species and pH values in background water are summarized in Table 1.

2.2. Remediation

The first remedial actions consisted in excavation and off-site disposal of oil-soaked surface soils. 19 monitoring wells were installed within two months, and the site was characterized in detail by hydrogeological and geophysical methods. The presence of Light Non Aqueous Liquid Phase (LNAPL) was observed in three monitoring wells 2.5 months after the spill and a dissolved plume was detected thereafter. Subsequently, 17 new wells devoted to hydraulic plume management and 30 more wells for tentative LNAPL recovery or monitoring were then installed (Fig. 1, information about the wells named throughout the paper in Table S1, Supp. Mat). Recovery wells were equipped with an electric submersed pump positioned deep below water table delivering continuously 0.5 to 2 m^3 h^{-1} of groundwater, and a pneumatic pump just below the water table filled gravitationally by LNAPL. This latter was delivered by pressurized air in cycles to a recovery tank. Recovery started in January 2010 in three wells and was extended progressively as a function of LNAPL arrival in other wells. LNAPL recovery was operated in a maximum of 22 wells until the end of March 2014. A total of 37 m^3 of LNAPL was recovered from the aquifer within four years. Water pumped in recovery wells, together with 20–25 m^3 h^{-1} pumped downgradient of the site to cut the dissolved plume, was mixed in an oil separator, analyzed weekly, treated by an activated charcoal filter and re-injected upgradient in seven wells.

2.3. Routine monitoring and targeted sampling campaigns

The routine site monitoring requested by authorities included a monthly survey of piezometric heads, basic water quality parameters (T, O_2, pH, EC) and hydrocarbons in 17 monitoring wells positioned all outside, downgradient and upgradient of the source zone. These monitoring wells included Pz4 and Pz17 (Fig. 1) and 15 other wells distant from 50 to 700 m of the border of the source zone (not pictured in Fig. 1). This monitoring was completed by a bi-weekly hydrocarbon analysis (BTEX, aliphatics C5–C35, other aromatics) of the pumped water at the inflow and the outflow of the activated charcoal filter. For both monthly and weekly monitoring, hydrocarbon analyses were performed by an accredited lab (Eurofins) by GC–MS.

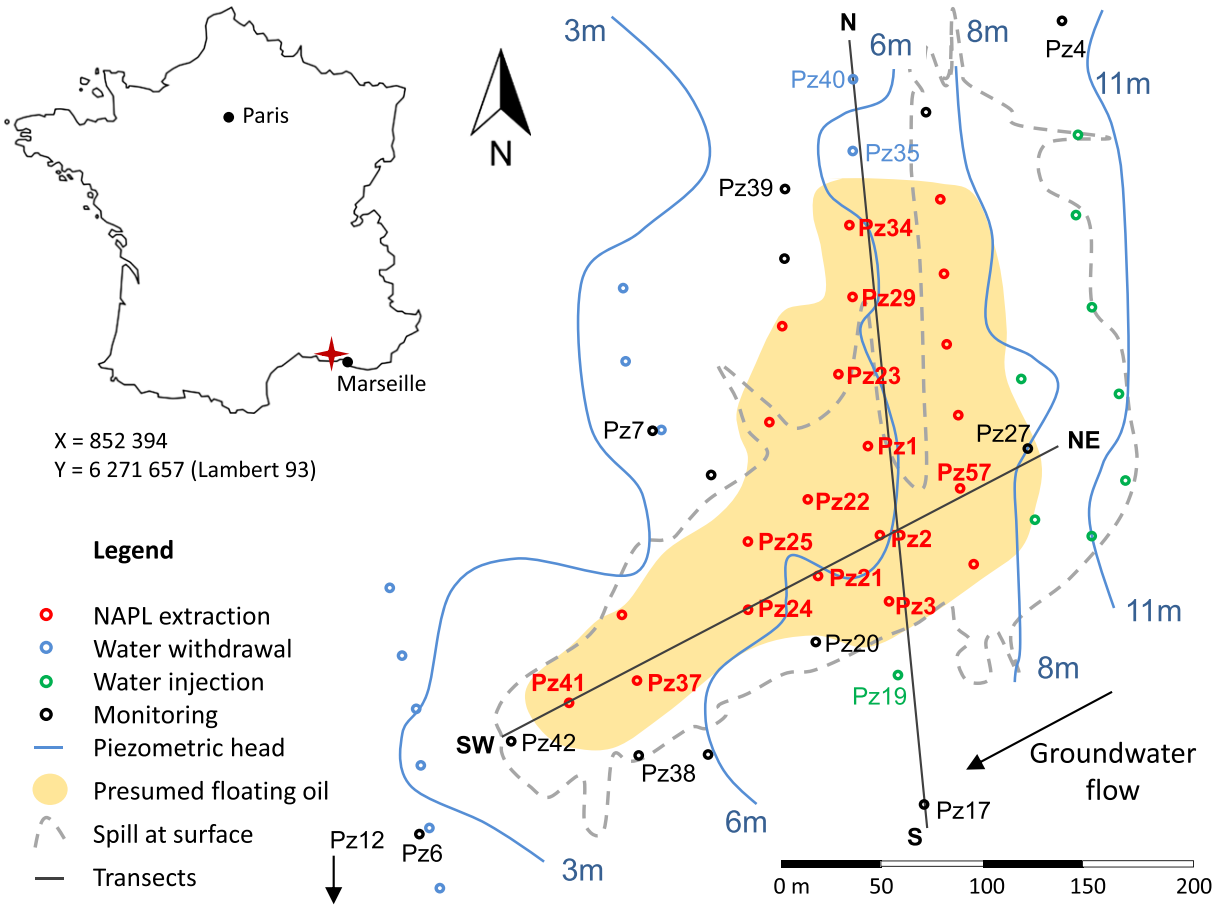

Fig. 1. Site location in France (left) and site map (right) showing water and LNAPL recovery facilities and the piezometric surface as observed on April 2, 2013. Blue wells belong to the hydraulic barrier and green wells to the injection line upgradient. Only wells of interest for this study are named. The dark gray line represents one of the transects along which wells were sampled during campaigns. The arrow shows Pz12, a monitoring well located approximately 110 m SW compared to Pz6, and outside of the figure.

In addition to this routine monitoring, seven targeted sampling campaigns were made in wells from within the source zone in order to measure a complete set of dissolved inorganic and organic species in groundwater to get a picture of ongoing geochemical processes. Some monitoring wells were also included (Pz4 and Pz17). Two of these campaigns included the analysis of stable carbon isotopes in hydrocarbons. These targeted seven sampling campaigns were made between April 2010 and December 2013, approximately every six months, during high flow and low flow conditions. Wells were sampled along two transects crossing the source zone, one oriented NS and the other oriented NE–SW (Fig. 1). The Results section includes either data from only the NS transect (cross-sectional transect) or data from both transects (maps).

Table 1
pH and concentrations of aqueous species in background well Pz4 from four sampling campaigns. DL: detection limit.

	35 months	41 months	47 months	52 months	Unit
pH	7.33	7.30	7.34	7.34	–
Dissolved oxygen	9.36	9.50	9.48	9.55	mg L^{-1}
NO_3^-	8.95	10.07	11.00	9.42	mg L^{-1}
Fe^{2+}	<DL[a]	<DL	<DL	<DL	mg L^{-1}
Mn^{2+}	<DL[b]	<DL	<DL	<DL	mg L^{-1}
SO_4^{2-}	66.6	72.5	78.2	69.7	mg L^{-1}
CH_4	<DL[c]	<DL	<DL	<DL	mg L^{-1}
Ca^{2+}	89.6	97.6	109.6	99.2	mg L^{-1}
Mg^{2+}	4.31	4.78	6.90	6.21	mg L^{-1}
K^+	0.61	0.61	0.58	0.50	mg L^{-1}
Na^+	9.95	12.15	11.18	12.53	mg L^{-1}
HCO_3^-	189	186	188	182	mg L^{-1}
Cl^-	18.6	21.5	22.3	20.1	mg L^{-1}

[a] 0.01 mg L^{-1}.
[b] 0.05 mg L^{-1}.
[c] 0.01 mg L^{-1}.

2.4. Sampling

For both routine monitoring and targeted sampling campaigns, groundwater samples in monitoring wells were obtained using a submersible electric pump Twister and a polyethylene tube (SDEC, France). At least two well volumes were pumped before sampling, recording continuously electric conductivity, temperature, pH and oxygen (WTW, Weilheim, Germany). Samples were taken only upon stabilization of these parameters. In recovery wells (sampled only during the targeted campaigns), water samples were obtained at each well from a tap on the hard PVC tubing used for pumping groundwater to the treatment facility.

Samples intended for cation analyses were filtered through 0.45 μm PTFE filters in glass amber bottles and were immediately acidified (1% hydrochloric acid Ultrapure TraceMetal Grade 34–37%, Fisher Scientific). Samples for anion analyses were filtered in HDPE bottles. For methane analysis and also for two sampling campaigns for stable carbon isotopes after 16 and 43 months, acidified glass amber bottles of 40 mL were filled and were capped thereafter without permitting air bubbles. Sampling vials for headspace analysis of BTEX were filled with 10 mL of groundwater and were immediately crimped.

2.5. Water and gas analyses for samples of the targeted campaigns

Anions (F^-, Cl^-, NO_3^-, NO_2^-, SO_4^{2-}, PO_4^{3-}) were analyzed by ion chromatography using a Dionex ICS-3000 instrument. Major cations (K^+, Na^+, Ca^{2+}, Mg^{2+}) and total soluble iron and manganese were analyzed by atomic absorption spectroscopy using a Thermo Scientific ICE 3000 Series instrument. Alkalinity was measured by titration using the Gran plot method (Gran, 1950). Dissolved Inorganic Carbon (DIC) was calculated from alkalinity and pH. The consistency of analytical data was checked by ion balances which showed generally below 5% error. BTEX were analyzed by gas chromatography with flame ionization detector (GC-FID) using a Perkin Elmer Clarus 580. Sampling was made with a TurboMatrix headspace sampler HS-40 (Perkin Elmer Inc., USA). Quantification was made with both internal and external standards. Methane was analyzed by GC-FID using a Varian 3800 instrument. A few mL of water were retrieved with a needle passed through the septum to create a headspace. 100 μL of this headspace were then sampled and manually injected. The detection limit for dissolved methane was 0.01 mg/L. Further details about analyses described in this section are given in (Ponsin et al., 2014b).

Stable carbon isotope analyses were made at the University of Neuchâtel, Switzerland. Measurements for enrichments in ^{13}C-BTEX were carried out by gas chromatography isotope-ratio mass spectrometry (GC-IRMS) using a gas chromatograph (Trace GC; Thermo Finnigan; Waltham, MA) connected via a combustion interface (Thermo Combustion III; Thermo Finnigan) to an isotope-ratio mass spectrometer (Delta plus XP; Thermo Finnigan). Oil-saturated water by equilibration with crude oil sampled on site 12 months after the spill was the source used for δ^{13}C comparison. The relative measure delta δ^{13}C (‰) for the source and the samples were calculated following Eq. (1):

$$\delta^{13}\mathrm{C}\ (‰) = \frac{R_{sample} - R_{standard}}{R_{standard}} \cdot 1000 \quad (1)$$

with R_{sample} being the $^{13}C/^{12}C$ ratio of the sample, and $R_{standard}$ the abundance ratio of the international standard (VPDB), both determined by isotope ratio mass spectrometry.

3. Results

3.1. Evolution of hydrocarbon concentrations

Results focus on benzene, which is the compound of particular concern in this study due to its toxicity and high mobility (known human carcinogen, Badham and Winn, 2007). Benzene concentration and piezometric heads in monitoring wells Pz6, Pz12 and Pz7 located downgradient of the oil body are shown in Fig. 2 (location of these wells on Fig. 1). They were chosen because they were among the first wells to be drilled downgradient and groundwater monitoring started only a few days after the spill. Benzene concentrations and piezometric head followed the same trend in the three wells. Concentrations of benzene in Pz6 started to increase about three months after the spill and half a month after free phase was observed in some wells upgradient (Fig. 2A). After peaking at approximately 500 μg L^{-1}, concentrations decreased after the implementation of the hydraulic barrier. A small but significant rebound was observed after 28 months, after a rapid rise of the water table to the annual maximum. Benzene concentrations and piezometric heads followed the same pattern in Pz12 and Pz7 than in Pz6, but benzene concentrations showed less variation between two measurements in Pz12 than in Pz6 and Pz7 (Fig. 2B, C).

Piezometric heads showed larger variations in Pz7 and Pz6 than in Pz12. Benzene concentrations in Pz12 and Pz7 started to increase about 136 days after the spill, and 59 days after free phase was observed. They reached 400 μg L^{-1} in Pz12 and 1200 μg L^{-1} in Pz7. No rebound in benzene was observed in December 2011 in Pz12.

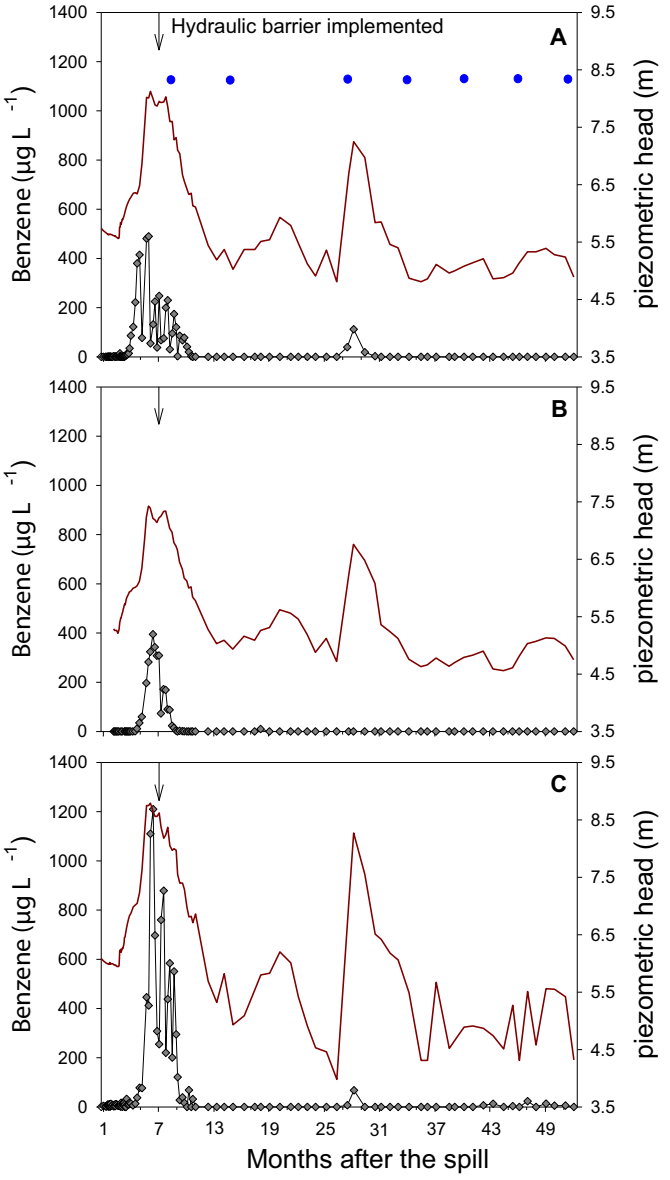

Fig. 2. Benzene concentration (gray diamonds) and piezometric head (dark red line) measured in Pz6 (A), Pz12 (B), and Pz7 (C) after the spill. Blue dots stand for sampling campaigns for detailed geochemical investigations.

Oxygen concentrations were initially always measured when benzene was monitored, and results are shown in Figure S1. In all wells, oxygen was initially between 8 and 10 mg L^{-1} and quickly dropped when benzene traces were monitored. Oxygen monitoring was discontinued in these wells thereafter.

Benzene concentrations measured at the inflow of the activated charcoal filter and in some wells of the source zone sampled during the targeted campaigns and belonging to the two transects are shown in Fig. 3. Concentration measured at the inflow represented an average concentration of benzene. Initially around 900 μg L^{-1}, concentrations decreased to <20 μg L^{-1} until month 28, when a rebound was observed with concentrations of up to 400 μg L^{-1}. Benzene concentrations decreased thereafter again and remained <10 μg L^{-1} after 34 months. Measurements of benzene concentrations within the source zone during the sampling campaigns after 15 and 28 months showed great variability (Fig. 3), with values ranging from 50 μg L^{-1} (Pz42) to 800 μg L^{-1} (Pz22). The concentration at the inflow of the activated carbon filter after 28 months were lower (<20 μg L^{-1}) and was in good agreement

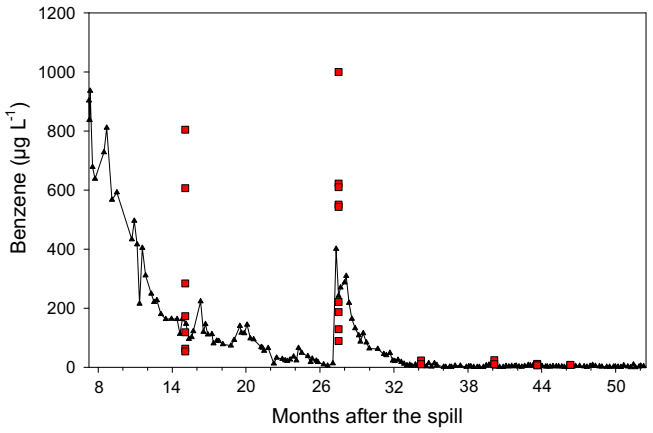

Fig. 3. Benzene concentrations measured at the inflow of the activated charcoal filter from the implementation of the treatment facilities to the end of 2013. Water pumped in different wells of the source zone is mixed before being treated, so the concentration measured at the inflow of the filter is an average concentration of benzene throughout the source zone. Red squares represent benzene concentration measured in individual wells with floating LNAPL during some of the sampling campaigns.

with concentrations measured in groundwater samples throughout the site. Concentrations of ethylbenzene and total xylenes measured at the inflow of the activated charcoal filter followed the same trend as benzene with a rebound after 28 months, but showed greater variability (Supp. material, Fig. S2). In contrast, toluene concentrations decreased toward detection limit within 24 months and showed no rebound after 28 months. Concentrations of total hydrocarbons (THC) C5–C10 also decreased until month 28, followed by the rebound between month 28 and the end of month 29 (Supp. material, Fig. S3). Concentrations of THC C10–C40 were generally <2 mg L^{-1} with peaks of up to 100 mg L^{-1}, which is above maximum solubility and suggests that groundwater contained temporarily suspended oil drops.

3.2. Evolution of electron acceptor (EA) concentrations

Concentrations of dissolved oxygen (DO), nitrate, and dissolved iron and manganese measured along the NS transect during the seven sampling campaigns are shown in Fig. 4. Upgradient and downgradient of the oil body, concentrations of DO ranged from 7 mg L^{-1} to 8.5 mg L^{-1} and were close to saturation (Fig. 4A). Beneath the oil body, they were often <0.1 mg L^{-1} and always below 2 mg L^{-1}, with a small rebound at 3 mg L^{-1} around 140 m (Pz1) during the first two campaigns. Nitrate concentrations were comprised between 10 mg L^{-1} and 12 mg L^{-1} on both sides of the oil body and decreased beneath the oil body (Fig. 4B). Concentrations of both dissolved iron and manganese were always below detection limits (0.15 mg L^{-1} for iron and 0.08 mg L^{-1} for manganese) outside of the oil body whereas they were of up to 6.5 mg L^{-1} across the transect in the heart of the contaminated area 28 months after the spill (2.8 mg L^{-1} of iron and 3.6 mg L^{-1} of manganese, Fig. 4C). They tended to decrease in the last campaigns and were below 2.2 mg L^{-1} 52 months after the spill. The campaign made after 28 months showed more reduced conditions compared to other campaigns with very low concentrations of DO and nitrate and the highest concentrations of dissolved iron and manganese.

Contour maps of sulfate concentrations during the five last campaigns are shown in Fig. 5. Not enough data were available from the first two campaigns (8 and 15 months) to draw such maps, but depletion in sulfate was observed in sampled wells. Pz2, Pz21 and Pz25 displayed sulfate concentration of approximately 20 mg L^{-1} eight months after the spill, and Pz22, Pz24 and Pz37 showed sulfate concentration <4 mg L^{-1} 15 months after the spill. The same pattern of sulfate concentrations was observed in all campaigns, with the most reduced area around Pz21, Pz24 and Pz25 (sulfate concentrations <10 mg L^{-1}). This area seemed to shrink 41 and

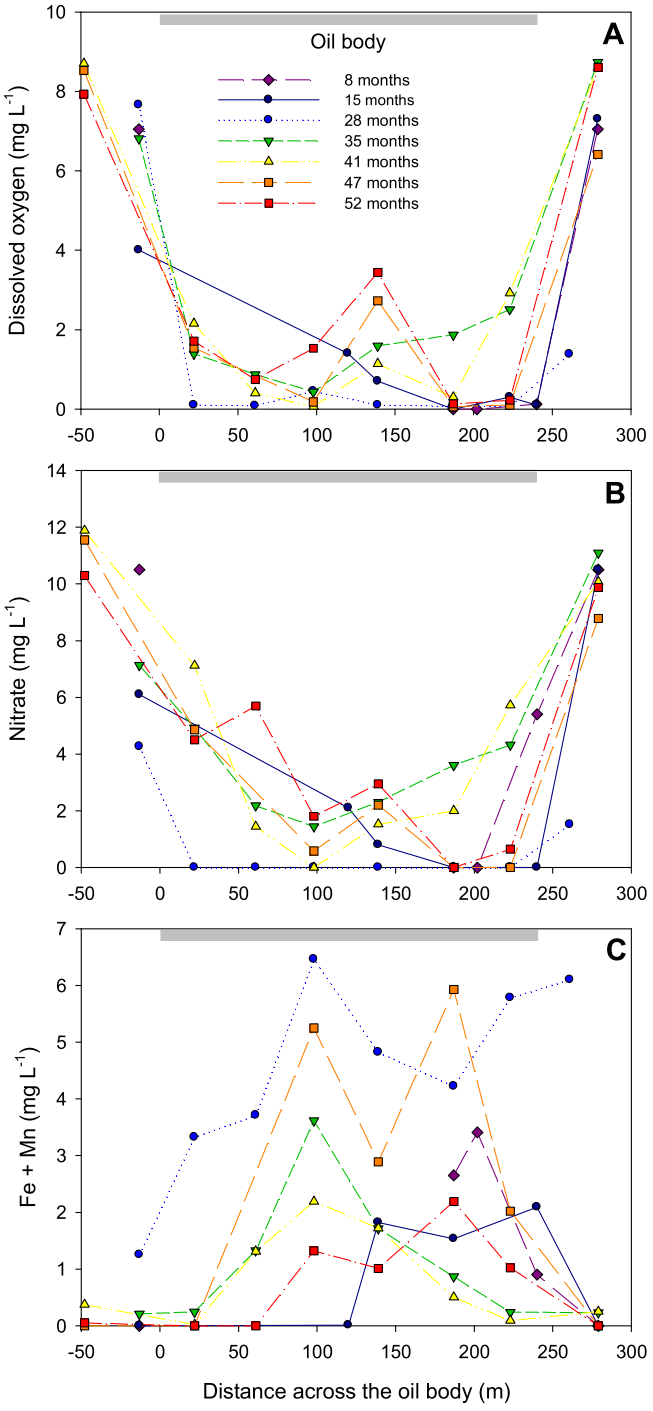

Fig. 4. Concentrations of dissolved oxygen (A), nitrate (B), and dissolved iron + manganese (C) measured during 7 sampling campaigns across the transect from N to S depicted in Fig. 1. Negative distances stand for wells located on northern margin of the source zone in the pristine area. Gray rectangles represent the extent of the oil body.

47 months after the spill (Fig. 5C, D). The map drawn with data from the campaign made after 28 months shows the largest area depleted in sulfate, and concentrations were below detection limit (0.7 mg L^{-1}) in several wells (Fig. 5A).

3.3. Carbon species

Contour maps of dissolved methane concentrations during the five last campaigns are shown in Fig. 6. Methane was not detected in wells monitored during the first two campaigns. After the first detection 28

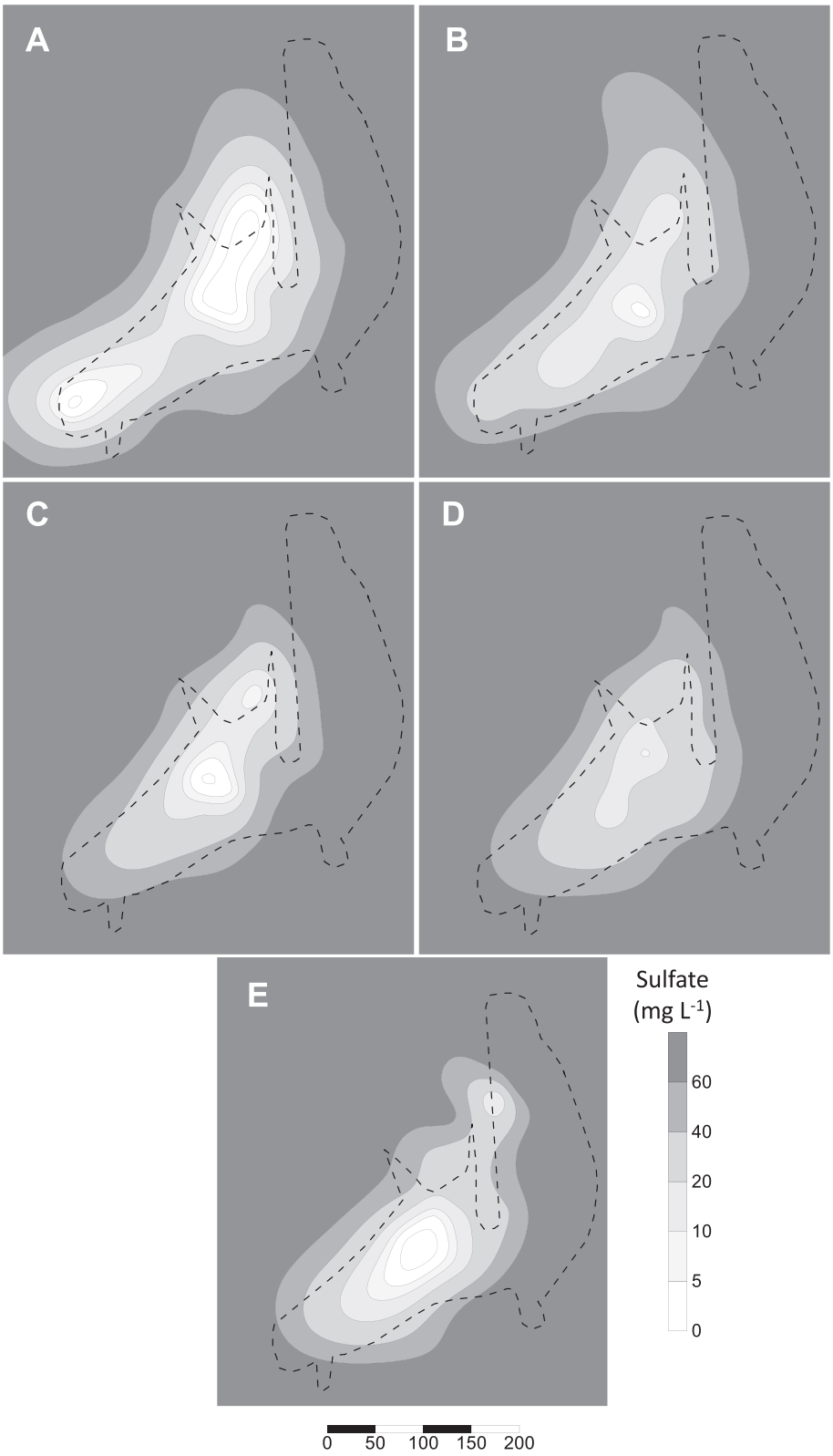

Fig. 5. Contour maps of sulfate concentration on site 28 months (A), 35 months (B), 41 months (C), 47 months (D) and 52 months (E) after the spill. The black dashed line represents the impacted area on the surface.

months after the spill, methane concentrations approximately doubled every six months and the methanogenic zone continuously enlarged during the monitoring period. Maximum measured concentrations ranged from 0.76 mg L^{-1} in Pz25 after 28 months (Fig. 6A) to 12 mg L^{-1} in Pz21 after 52 months (Fig. 6E). These two wells do not belong to the transect.

Concentrations of methane, dissolved inorganic carbon (DIC), and BTEX along the NS transect are shown in Fig. 7. Methane concentration

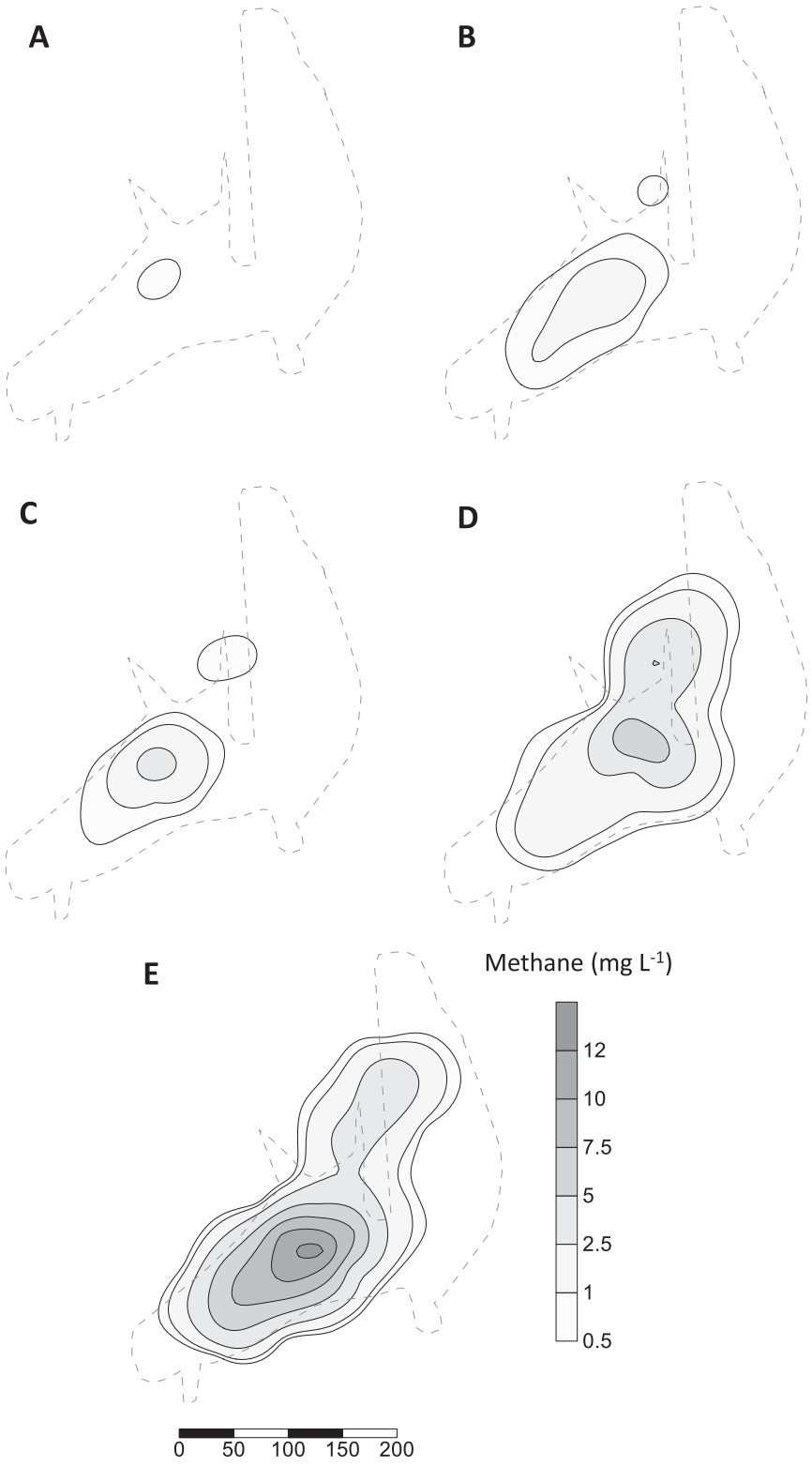

Fig. 6. Contour maps of methane concentration on site 28 months (A), 35 months (B), 41 months (C), 47 months (D) and 52 months (E) after the spill. The gray dashed line represents the impacted area on the surface.

continuously increased within the contaminated area, and this increase was more significant between months 41, 47 and 52 (Fig. 7A). Concentrations of DIC were <4.3 mM outside of the oil body whereas they were comprised between 4.3 mM and 7 mM in the heart of the contaminated area (Fig. 7B). The highest concentrations were measured during the campaign made after 28 months, with DIC of up to 11.1 mM around 98 m (Pz23). BTEX concentrations (sum of concentration of benzene, toluene, ethylbenzene, and total xylenes) were below detection limit upgradient and downgradient of the oil body and greatly varied within the contaminated area (Fig. 7C). Generally, they tended to decrease with time. The highest concentrations were measured during the campaign made after 28 months.

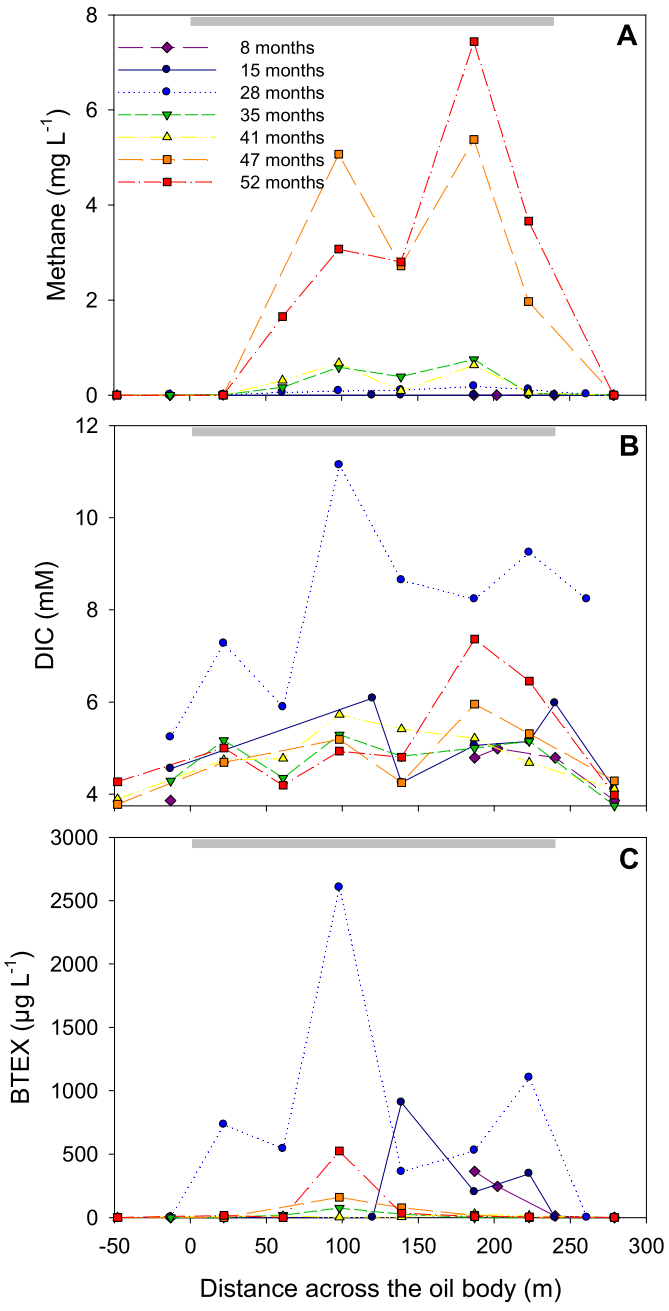

Fig. 7. Concentrations of methane (A), DIC (B), and BTEX (C) measured during the sampling campaigns across the transect from N to S depicted in Fig. 1. Negative distances stand for wells located on northern margin of the source zone in the pristine area. Gray rectangles represent the extent of the oil body.

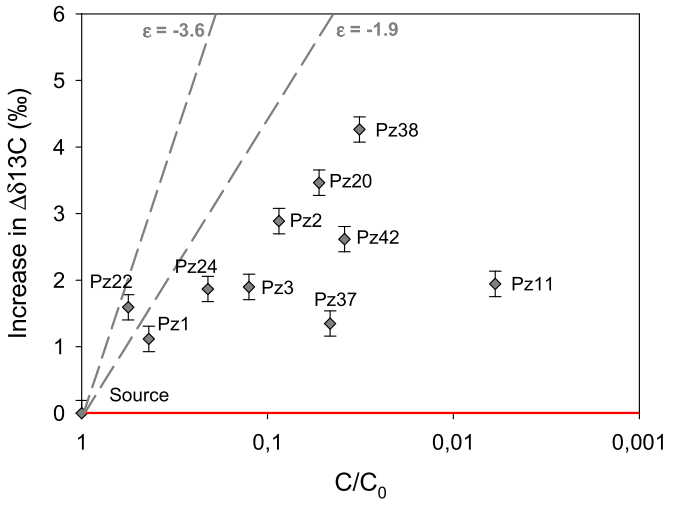

Fig. 8. Isotope plot of field benzene isotope data after 16 months. The gray dashed lines correspond to the expected isotope evolution if benzene concentrations were affected by biodegradation only (highest and lowest ε found in literature for sulfate reduction, Aelion et al., 2010), the red line if they were affected by dilution only. Each point is an average of duplicate analysis and the error bar represents the analytical standard error (0.19‰, n = 6).

3.4. Carbon isotopes in hydrocarbons

Fig. 8 shows, after 16 months, the difference in isotope ratio $\Delta\delta^{13}C$ (‰) for benzene between the value for each well sampled and the source, as a function of C/C_0, with C_0 benzene concentration of the source. $\Delta\delta^{13}C$ was inversely correlated to C/C_0, with values of $\Delta\delta^{13}C$ increasing when C/C_0 decreased. The same correlation is observed for ethylbenzene, *n*-pentane and *n*-hexane isotope ratio $\Delta\delta^{13}C$ as a function of C/C_0 (Supp. mat Fig. S4). Toluene was detected in only two wells after 16 months, but the shift in $\delta^{13}C$ was significant, with a maximum $\Delta\delta^{13}C$ of 5.51 ± 0.22‰ for Pz24. Isotope enrichment for *m* and *p*-xylenes was <0.8‰, except for 2 wells (0.85 ± 0.23‰ in Pz22 and 1.18 ± 0.23‰ in Pz20), whereas *o*-xylene was below detection limit in most wells. Isotope data from the sampling campaign after 43 months did not show significant shift in $\delta^{13}C$ value for targeted compounds and the measured concentrations of BTEX were at least one order of magnitude lower than during the first campaign (data not shown).

4. Discussion

4.1. Temporal geochemical evolution of the source zone

Benzene appeared in significant concentrations after 4–5 months in the three monitoring wells drilled right after the spill (Fig. 1). The arrival was slightly preceded by a drop in oxygen concentrations after 3–4 months (Fig. S1). Additional measurements in the source zone (data not shown) confirmed also a general decrease of oxygen concentrations, but drilling operations and flow changes due to the operation of the hydraulic barrier made it difficult to interpret data. The first complete sampling campaign under steady pumping regime, eight months after the spill, showed that several wells beneath the oil body were depleted in nitrate and sulfate, with higher concentrations of dissolved iron and manganese than outside of the oil body. This suggests that anaerobic degradation processes, from denitrification to sulfate reduction, appeared on site within eight months. Data showed that the most reducing area was located around Pz21 and Pz25 (Fig. 1), with the highest depletion in sulfate measured for each campaign (Fig. 5), and the highest concentrations of ferrous iron measured in Pz25 (of up to 7.6 mg L^{-1} of Fe^{2+} after 28 months). Methane was detected in this area for the first time after 28 months, and the highest concentrations of methane during the different campaigns were always measured in this area (Fig. 6). A dipole test with injection and recirculation of nutrients (nitrate and phosphate) was conducted in Pz21 and Pz25 between months 21 and 25 after the spill (Ponsin et al., 2014a). Dissolved nitrate and phosphate decreased rapidly to non-detectable concentration after month 26 in this zone.

In a microcosm study set up with material from this site, redox conditions shifted from aerobic degradation to methanogenesis in approximately 200 days (Ponsin et al., 2014b). The appearance of methane at the field site took much longer compared to the microcosm, but may seem quite fast compared to the similar pipeline rupture in Bemidji, where methane was detected for the first time on site five years after the spill. Background concentrations of dissolved EA, especially nitrate

and sulfate, were much lower in Bemidji than in the La Crau aquifer (0.2 mg L^{-1} of nitrate, 2.3 ± 0.2 mg L^{-1} of sulfate (Baedecker et al., 1993)). However, average 0.5 M HCl-extractable Fe(III) in Bemidji (23.8 ± 2.0 μmol g^{-1} sediment, (Tuccillo et al., 1999)) was approximately three times higher than in the La Crau aquifer (8.6 ± 0.1 μmol g^{-1} sediment, (Ponsin et al., 2014b)). At Bemidji, iron reduction is the most important redox process, and the higher content of microbially available ferric iron in sediments retarded the onset of methanogenesis. In the microcosms with Crau sediments, the ratio of solids to groundwater was low, and iron oxides were depleted faster than at the field site.

At the Crau site, the most reducing conditions were observed after 28 months, with an enlarged area depleted in DO, nitrate, sulfate and higher concentrations of dissolved iron and manganese. This campaign was made during a major rise of water level after one year of low water level (Fig. 2A), and coincided with a rebound in benzene concentrations measured in monitoring wells Pz6 and Pz7 (Fig. 2A, C), and at the inflow of the activated charcoal filter (Fig. 3). Previous studies (Dobson et al., 2007; Anderson et al., 1992) showed that water-table fluctuations lead to an extended entrapment of LNAPL below the water table and to an increased LNAPL/water interfacial area, promoting thus an enhanced dissolution and enhanced biodegradation. At the la Crau site, most LNAPL reached the free water table when it was high in winter 2010. Later, the water table sunk and created a smear zone with entrapped LNAPL. This entrapped LNAPL was again below the water level in November 2011, explaining the observed rebound of benzene, ethylbenzene and xylenes concentrations (Figs. 3. and Fig S2. B and C. from Supp. Mat.). Higher availability in dissolved hydrocarbon lead to an enhanced biodegradation and thus to the strong reducing conditions observed during this campaign.

4.2. Spatial evolution of geochemistry

The profiles of dissolved electron acceptors across the source zone show a clearly fringe-dominated consumption of oxygen and nitrate, although an exception occurred in one well in the center of the plume where DO and NO_3^- concentrations were higher than elsewhere in the oil zone. The disappearance of O_2 and NO_3^- at the fringes is in accordance with literature postulating a fringe-controlled degradation of hydrocarbon plumes (Borden and Bedient, 1986; Atteia and Guillot, 2007). In contrast, iron, sulfate, and methane concentrations along transects suggest a core degradation of hydrocarbons. This core degradation gains importance with the onset of anaerobic conditions later than 28 months after the spill and is well reflected also by highest DIC concentrations in the center of transects at these dates. Future modeling of the plume should be based on models that include both, core and fringe degradation (Gutierrez-Neri et al., 2009; Hunkeler et al., 2010), or numerical models accounting for all degradation processes in a thermodynamically-governed sequence.

4.3. Hydrocarbon degradation

The theoretical maximum solubilities for benzene and toluene in water equilibrated with the original crude oil according to Raoult's law are calculated to be of 2700 μg L^{-1} for benzene and 1800 μg L^{-1} for toluene (0.06% w/w benzene and 0.17% w/w toluene in the spilled oil). However, experimental data showed that these values were never reached at any point at the field site. A sample of oil taken in august 2010 from the LNAPL recovery system was equilibrated with water and this resulted in a solubility of 1200 μg L^{-1} for benzene and 200 μg L^{-1} for toluene. Two processes can explain the markedly lower concentrations in groundwater compared to theoretical solubilities: first, the oil bursting to the surface after pipeline break in august 2009 during a hot summer weather period underwent volatilization after the spill before it started to infiltrate, and partly lost the most volatile compounds, among them BTEX. Second, dissolution enhanced by biodegradation in the saturated zone furthermore depleted the crude oil in these two compounds. It must be noted here that pure dissolution not enhanced by biodegradation would deplete benzene three times faster than toluene from the source zone because of a three-fold higher solubility of benzene. Our results in Figs. 3 and S2 (Supp. mat) suggest the inverse: that toluene was much faster depleted and reached much earlier very low dissolved concentrations in groundwater than benzene. This suggests that toluene is well degraded on site and that degradation started early after the spill. For benzene, the situation is less clear based on concentration measurements. Sharp increases of benzene concentration in Pz6, Pz7 and Pz12 suggested that benzene degradation had either not started yet 6 months after the spill or was masked by other processes (Fig. 2): benzene concentrations reached the maximum values in Pz7 in mid-February 2010. The decrease in benzene concentrations after mid-February 2010 is due to the implementation of the hydraulic barrier that cut the plume, which never reached Pz6 or Pz7 again, except when water level dramatically rose in November 2011. Benzene was then degraded before reaching Pz12 since it was not detected in this well (Fig. 2B). However, the general trend of dissolved benzene concentrations showed also a marked decrease during the four-year period studied, suggesting that physical and tentatively biological natural attenuation was very effective on the site. Complementary field and lab data confirm that benzene concentrations were rapidly lowered to below detection limit in a field test and in microcosms where nitrate and phosphate were added (Ponsin et al., 2014a, 2014b).

Further strong evidence for toluene and benzene biodegradation is given by the results of carbon isotope ratios in these compounds. Both compounds undergo significant isotopic enrichment along flow paths in the source zone. Recent studies showed that physical processes such as sorption and diffusion could lead to isotope fractionation and to an overestimation of biodegradation, although the importance of these processes in the field has not been shown yet (for a review, see Braeckevelt et al., 2012). Using a model indoor aquifer and a transient toluene pulse, Qiu et al. (2013) were able to determine a specific isotope enrichment factor attributable to sorption only and accounting for about 15% of the isotope enrichment factor attributable to biodegradation only. However, the la Crau aquifer has a low content of organic matter and the plume was more or less in a steady-state, so sorption in the fringe of the plume is most probably negligible. Labolle et al. (2008) showed through mathematical simulations that diffusion can control contaminant transport at low flow velocity. They suggested that diffusive isotope fractionation could be in the same order of magnitude as isotope fractionation due to biodegradation in transport regimes where diffusive mass transfer between high and low-permeability zones is prominent during transient state plume evolution. In the case of the Crau site, the existence of such a mass transfer is unknown, but at the time of isotope analysis, the plume had reached steady state and therefore diffusion can be excluded as fractioning process.

The observed enrichment can be used for a quantitative assessment of degradation provided that an enrichment factor ε is known. However, the values for isotope enrichment factors for each compound are somewhat variable, because the mechanism of the initial transformation step on site under different redox conditions are variable. An isotope enrichment factor can be estimated from the data by plotting ln (R/Ri) versus ln (C/Ci) for each compound, with Ci the concentration of the compound in the source, and $R = \delta^{13}C + 1000$. The isotope enrichment factors calculated from the data are −0.9, −1.2 and −0.9 for benzene, ethylbenzene and *n*-pentane, respectively. No estimations could be given from the data for toluene and *n*-hexane. However, these estimations from field data are affected by both degradation and dissolution and they would lead to an underestimation of biodegradation. Many wells are in the source and hence benzene will be re-dissolved. The isotope shift would then be the net effect between biodegradation and re-dissolution. The fact that it is still possible to see a shift suggests that biodegradation is quite strong and/or mass transfer from the NAPL is limited.

Another estimation of ε can be tempted given that predominant redox conditions on site are known (see Section 4.4). For each compound, isotope enrichment factors from previous studies were compiled (Aelion et al., 2010). Only studies under sulfate-reducing conditions were taken into account, or under anaerobic conditions if ε values for sulfate reduction were not available. Provided that an averaged isotope enrichment factor associated to degradation is known, the fraction of compound that is degraded (*fdeg*) can be estimated from isotope data (Aelion et al., 2010):

$$fdeg = \exp\left(\frac{\Delta\delta^{13}C}{\varepsilon(‰)}\right) \quad (2)$$

with $\Delta\delta^{13}C$ the difference in isotope ratio between the well sampled and the source expressed in ‰. This fraction can also be expressed as a percentage of degradation *B* (Meckenstock et al., 2004):

$$B = 100(1-fdeg). \quad (3)$$

B corresponds to the concentration reduction compared to the expected concentration if dilution only occurred; the remaining percentage (1-B) is due to dilution and dispersion.

The estimated percentages of degradation for several compounds are compiled in Table 2. For toluene, the percentage of degradation was >75%, which is consistent with the very low concentration observed at the inflow of the activated charcoal filter and the quick drop to undetectable level. Wells within the most reduced area (Pz1 to 3, Pz22 and Pz24) tended to display the smallest percentage of biodegradation while wells at the plume fringe (Pz20, Pz38 and Pz42) showed the highest percentage of biodegradation for the studied compounds.

A previous study in microcosms (Ponsin et al., 2014b) showed that BTEX were degraded even under methanogenesis, but at a slower rate compared to other redox conditions. The absence of significant shift in $\delta^{13}C$ after 43 months may be due to the continuous input of the targeted compounds by the dissolution of free phase that could mask isotope fractionation associated with biodegradation.

4.4. Carbon fluxes

Carbon fluxes in kg C day^{-1} were determined from data obtained from each campaign to assess the flux of DIC caused by hydrocarbon biodegradation across the transect N to S. The surface of this transect was assessed by multiplying the length of the transect between two sampled wells by the wetted cross section in gravel deposits. Fluxes were obtained by multiplying this surface by the natural Darcy velocity (0.32 m day^{-1}, estimated from an effective velocity comprised between 2.4 and 2.7 m day^{-1} and a porosity comprised between 0.1 and 0.15) and by the measured DIC value to which background DIC value was previously subtracted. It is worth noting that the hydraulic containment with water pumping and reinjection has little impact on the calculated fluxes: water reinjected upgradient is free from dissolved EA and hydrocarbons after treatment by the activated charcoal filter. However, inorganic carbon concentration might be increased in injected water, and therefore an overestimation of carbon production in the transect is possible. The additional flow created by the recirculation of water increased the dissolution of LNAPL and is thus taken into account in the estimation of organic carbon fluxes.

Carbon fluxes for each campaign are shown in Fig. 9. The organic carbon fluxes are not shown in Fig. 9 because they are almost negligible (maximum of 0.3 kg C/day right after the implementation of the hydraulic barrier). A hypothetic inorganic carbon production from EA consumption was also determined with carbon production rates summarized in Table 3. Results are also shown in Fig. 9. For each campaign, the carbon flux estimated from DIC values was slightly higher than the flux estimated from EA consumption. Concentrations of Ca^{2+} and Mg^{2+} in wells beneath the oil body were, respectively, 10 and 50% higher in average than outside of the oil body during the different campaigns, reflecting an increased dissolution of both magnesium carbonate and calcium carbonate in the contaminated area. The observed gap between the two estimations of inorganic carbon production for each campaign can be thus due to carbonate dissolution.

The carbon production estimated from DIC values 28 months after the spill was approximately eight times higher than the average production from the other campaigns. Carbon production from EA consumption was also the highest on that date, but not in accordance with real carbon production. Enhanced biodegradation due to a major rise in water level, lead to a drop in measured pH beneath the oil body. That pH was the lowest among all the campaigns, with a mean value of 6.8 while the mean value for other campaigns was comprised between 7.1 and 7.3. Calcium concentrations beneath the oil body were in average 22% higher than in background. Carbonate dissolution markedly increased during this campaign, explaining a dramatic increase in carbon production. The effects observed at 28 months after the spill are best explained by a combination of an important dissolution of soluble degradable hydrocarbons from oil droplets in the vadose zone combined with a mobilization of additional electron acceptors from the capillary fringe and even from above due to the sudden rise of the water table. Although carbon production estimated from DIC values decreased thereafter markedly, it tended to increase later again after 35 months.

4.5. Dominant redox processes

Estimations of carbon production for each campaign showed that the highest carbon flux was attributable to sulfate reduction (in average 60% of carbon production), which is therefore the predominant anaerobic biodegradation process for hydrocarbon removal. This proportion has been decreasing since December 2012, after 35 months, and the carbon production attributable to sulfate reduction was 50% after 52 months. Methanogenesis was responsible for 1% of carbon production 28 months after the spill when methane was first detected on-site. Contribution of methanogenesis in carbon production has been increasing ever since to reach 27% after 52 months. The core degradation processes dominate thus quantitatively at this site compared to fringe degradation with DO and nitrate.

Table 2
Estimation of percentage of degradation B for different compounds. Values between brackets stand for B estimated using the smallest/the highest ε found in the literature. The mean B was calculated with values from all the sampled wells. No mean was estimated for toluene, which was detected in only two wells.

Compound	Smallest–highest ε (‰)[a]	Well displaying the highest B (%)	Well displaying the lowest B (%)	Mean B (%)
Benzene	−1.9/−3.2	Pz38 (89.4/73.3)	Pz1 (44.4/29.2)	66.8 ± 14.5 48.9 ± 14.1
Toluene	−0.8/−2.8	Pz24 (99.9/86.0)	Pz22 (99.6/79.1)	–
Ethylbenzene	−2.1[b]	Pz2 (53.0)	Pz1 (15.3)	34.2 ± 16.4
n-Pentane	−2.3/−2.7[b]	Pz20 (73.2/67.4)	Pz22 (33.6/29.4)	57.2 ± 14.9 51.8 ± 14.3
n-Hexane	−1.6[b]	Pz22 (95.4)	Pz3 (64.2)	78.8 ± 15.4

[a] Compiled from Aelion et al (2010).
[b] Unspecified anaerobic conditions.

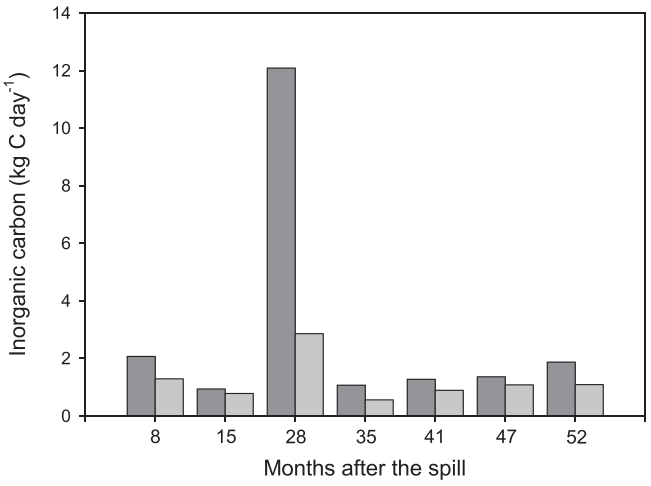

Fig. 9. Estimated carbon production: Dissolved Inorganic Carbon (DIC) flux caused by biodegradation and carbonate dissolution (dark gray) and hypothetic carbon production from EA consumption (light gray), in kg C day^{-1}.

For comparison, at the Bemidji spill site, concentrations of methane increased from almost zero to approximately 17 mg L^{-1} in the 2.5 years once methanogenesis started following the lag-phase of 5 years. Baedecker et al. (1993), Bennett et al. (1993) and Eganhouse et al. (1993) studied temporal changes in the Bemidji plume between 1986 and 1992 (i.e. between 7 and 13 years after the spill), and showed that predominant anaerobic processes were evolving with time from iron reduction to methanogenesis, and that the plume was becoming more reducing with time. In a survey of 38 sites, Wiedemeier et al. (1999) estimated that methanogenesis was responsible for 16% of petroleum hydrocarbon degradation, showing the relative importance of this degradation pathway for plume control.

4.6. Carbon mass balance

An attempt to quantify hydrocarbon oxidation can be made by using the fluxes of carbon produced from EA consumption. Within a time frame starting seven months after the spill and ending 53 months after the spill, a total of 2047 kg of hydrocarbons ($CH_{1.85}$) were degraded on site, to which 115 kg from a recirculating tracer test should be added (Ponsin et al., 2014a), for a total of 2162 kg (2.51 m^3). Within the same time frame, 900 kg of hydrocarbons (1.05 m^3) were trapped in the activated charcoal filter, and 30,616 kg (35.6 m^3) of LNAPL were recovered by skimming (unpublished classified report). A previous field study gave an estimated volume of residual crude oil below the capillary fringe of 309 ± 93 m^3, with a non-extractable oil volume of 142 ± 43 m^3 (Ponsin et al., in press).

The mass of oxidized hydrocarbon may seem low compared to the overall mass recovered by physical means. However, biodegradation is a more efficient process for plume control compared to pumping and filtration since it removed more than twice of dissolved hydrocarbons compared to the activated charcoal filter. Furthermore, biodegradation was probably underestimated since this mass balance did not take into account biodegradation in the vadose zone. There, oil can be degraded aerobically in the presence of O_2 (Amos et al., 2005), or anaerobically and in particular under methanogenic conditions (Bekins et al., 2005).

Table 3
Stoichiometric changes in concentrations of electron acceptors consumed or products formed for degradation of 1 mg/L hydrocarbon. The model hydrocarbon used for these estimations was $CH_{1.85}$ (Bolliger et al., 1999).

Electron acceptor/product	Equivalent change for 1 mg/L HC degraded
O_2	−3.4 mg L^{-1}
NO_3^-	−5.2 mg L^{-1-}
Fe^{2+}	+23.7 mg L^{-1+}
Mn^{2+}	+11.7 mg L^{-1}
SO_4^{2-}	−5.3 mg L^{-1-}
CH_4	+0.8 mg L^{-1}

5. Conclusions

Evolution of the hydrocarbon-degrading processes observed in the La Crau aquifer revealed the following picture: it took first about 2.5 months for the liquid crude oil to reach the groundwater table. Then during the following 3.5 months, the plume expanded and peak concentrations of BTEX were observed in wells beyond 200 m downgradient of the source zone after 6 months. Dissolved oxygen concentrations fell from initial 8–10 mg/L to low values in wells where BTEX appeared. After 8 months, geochemical parameters indicated a full expression of all aerobic and anaerobic natural attenuation processes except methanogenesis in the source zone. This latter process evolved progressively between months 28 and 48, at the expense of metal-reducing processes (Fe and Mn) which decreased in magnitude. Methanogenesis became the second most important process for hydrocarbon degradation on a mass balance after sulfate reduction, although the aquifer was initially aerobic and fast-flowing. Water pumping in the source-zone and biodegradation of dissolved compounds caused that the dissolved concentrations of toluene and benzene dropped markedly during the studied period.

This work focused on natural attenuation beneath the source zone: no permanent plume of dissolved HC has been observed so far, because of the hydraulic containment implemented seven months after the spill. The recent shutdown of the physical remediation techniques could lead to further expansion of the plume. The smear zone extends vertically over approximately 2.5 m, and only the lower part of this zone is almost always below the water table. Pulses of HC dissolution should be expected in the future, consequently to point rises of the water table. These fluctuations of water level should lead to variations of the plume length. A rapid establishment of methanogenic conditions could also have some impacts on its length: Cozzarelli et al. (2001) showed that, in Bemidji, the hydrocarbon plume was growing slowly as sediment iron oxides were depleted and the aquifer evolved from iron reducing to methanogenic conditions.

Work described in this paper is a strong basis to build a reactive transport model of the plume: first, under the influence of physical remediation, and then after the shutdown of all facilities. This model will be described in future work.

Acknowledgments

The authors gratefully acknowledge financial support by ICF Environnement, Société du Pipeline Sud-Européen and ADEME. We thank Carine Demelas and Laurent Vassalo for their technical assistance, and SERPOL for using their field facilities and for providing oil samples.

Appendix A. Supplementary data

Supplementary data to this article can be found online at http://dx.doi.org/10.1016/j.scitotenv.2015.01.033.

References

Aelion, C.M., Höhener, P., Hunkeler, D., Aravena, R., 2010. Environmental Isotopes in Biodegradation and Bioremediation. CRC Press (Taylor and Francis), Boca Raton.
Amos, R.T., Mayer, K.U., Bekins, B.A., Delin, G.N., Williams, R.L., 2005. Use of dissolved and vapor-phase gases to investigate methanogenic degradation of petroleum hydrocarbon contamination in the subsurface. Water Resour. Res. 41, W02001.
Anderson, M.R., Johnson, R.L., Pankow, J.F., 1992. Dissolution of dense chlorinated solvents into ground-water.1. Dissolution from a well-defined residual source. Ground Water 30, 250–256.
Atteia, O., Guillot, C., 2007. Factors controlling BTEX and chlorinated solvents plume length under natural attenuation conditions. J. Contam. Hydrol. 90, 81–104.

Badham, H.J., Winn, L.M., 2007. Investigating the role of the aryl hydrocarbon receptor in benzene-initiated toxicity in vitro. Toxicology 229, 177–185.
Baedecker, M.J., Cozzarelli, I.M., Siegel, D.I., Bennett, P.C., Eganhouse, R.P., 1993. Crude oil in a shallow sand and gravel aquifer — III. Biogeochemical reactions and mass balance modeling in anoxic ground water. Appl. Geochem. 8, 569–586.
Bekins, B.A., Godsy, E.M., Warren, E., 1999. Distribution of microbial physiologic types in an aquifer contaminated by crude oil. Microb. Ecol. 37, 263–275.
Bekins, B.A., Hostettler, W.N., Herkelrath, W.N., Delin, G.N., Warren, E., Essaid, H.I., 2005. Progression of methanogenic degradation of crude oil in the subsurface. Environ. Geosci. 12, 139–152.
Bennett, P.C., Siegel, D.I., Baedecker, M.J., Hult, M.F., 1993. Crude oil in a shallow sand and gravel aquifer — I. Hydrogeology and inorganic geochemistry. Appl. Geochem. 8, 529–549.
Bennett, P.C., Hiebert, F.K., Roberts Rogers, J., 2000. Microbial control of mineral–groundwater equilibria: macroscale to microscale. Hydrogeol. J. 8, 47–62.
Berard, P., Daum, J.R., Martin, J.C., 1995. "MARTCRAU": actualisation du modèle de la nappe de la Crau. Rapport BRGM R 38199. BRGM.
Bolliger, C., Höhener, P., Hunkeler, D., Häberli, K., Zeyer, J., 1999. Intrinsic bioremediation of a petroleum hydrocarbon-contaminated aquifer and assessment of mineralization based on stable carbon isotopes. Biodegradation 10, 201–217.
Borden, R.C., Bedient, P.C., 1986. Transport of dissolved hydrocarbons influenced by oxygen-limited biodegradation: 1. Theoretical development. Water Resour. Res. 22, 1973–1982.
Braeckevelt, M., Fischer, A., Kästner, M., 2012. Field applicability of Compound-Specific Isotope Analysis (CSIA) for characterization and quantification of in situ contaminant degradation in aquifers. Appl. Microbiol. Biotechnol. 94, 1401–1421.
Chaplin, B.P., Delin, G.N., Lahvis, M.A., Baker, R., 2002. Long term evolution of biodegradation and volatilization rates in a crude-oil-contaminated aquifer. Bioremediat. J. 6, 237–255.
Cozzarelli, I.M., Baedecker, M.J., Eganhouse, R.P., Goerlitz, D.F., 1994. The geochemical evolution of low-molecular-weight organic acids derived from the degradation of petroleum contaminants in groundwater. Geochim. Cosmochim. Acta 58, 863–877.
Cozzarelli, I.M., Bekins, B.A., Baedecker, M.J., Aiken, G.R., Eganhouse, R.P., Tuccillo, M.E., 2001. Progression of natural attenuation processes at a crude-oil spill site — I. Geochemical evolution of the plume. J. Contam. Hydrol. 53, 369–385.
Curtis, G.P., 2003. Comparison of approaches for simulating reactive solute transport involving organic degradation reactions by multiple terminal electron acceptors. Comput. Geosci. 29, 319–329.
Davis, P.M., Diaz, J.-M., Gambardella, F., Sanchez-Garcia, E., Uhlig, F., 2013. Performance of European Cross-country Oil Pipelines — Statistical Summary of Reported Spillages in 2012 and Since 1971. CONCAWE, Brussels.
Delin, G.N., Herkelrath, W.N., 2014. Effects of a dual-pump crude-oil recovery system, Bemidji, Minnesota, USA. Groundw. Monit. Remediat. 34, 57–67.
Delin, G.N., Essaid, H.I., Cozzarelli, I.M., Lahvis, M.H., Bekins, B.A., 1998. Ground Water Contamination by Crude Oil Near Bemidji. USGS Fact Sheet, Minnesota, p. 4.
Dobson, R., Schroth, M.H., Zeyer, J., 2007. Effect of water-table fluctuation on dissolution and biodegradation of a multi-component, light nonaqueous-phase liquid. J. Contam. Hydrol. 94, 235–248.
Eganhouse, R.P., Baedecker, M.J., Cozzarelli, I.M., Aiken, G.R., Thorn, K.A., Dorsey, T.F., 1993. Crude oil in a shallow sand and gravel aquifer — II. Organic geochemistry. Appl. Geochem. 8, 551–567.
Essaid, H.I., Bekins, B.A., Godsy, E.M., Warren, M.J., Baedecker, M.J., Cozzarelli, I.M., 1995. Simulation of aerobic and anaerobic biodegradation processes at a crude oil spill site. Water Resour. Res. 31, 3309–3327.
Essaid, H.I., Cozzarelli, I.M., Eganhouse, R.P., Herkelrath, W.N., Bekins, B.A., Delin, G.N., 2003. Inverse modeling of BTEX dissolution and biodegradation at the Bemidji, MN crude-oil spill site. J. Contam. Hydrol. 67, 269–299.
Fraser, M., Barker, J.F., Butler, B., Blaine, F., Joseph, S., Cooke, C., 2008. Natural attenuation of a plume from an emplaced coal tar creosote source over 14 years. J. Contam. Hydrol. 100, 101–115.
Gran, G., 1950. Determination of the equivalence point in potentiometric titrages. Acta Chem. Scand. 4, 559–577.
Gutierrez-Neri, M., Ham, P.A.S., Schotting, R.J., Lerner, D.N., 2009. Analytical modelling of fringe and core biodegradation in groundwater plumes. J. Contam. Hydrol. 107, 1–9.
Hiebert, F.K., Bennett, P.C., 1992. Microbial control of silicate weathering in organic-rich ground water. Science 258, 278–281.
Hunkeler, D., Höhener, P., Atteia, O., 2010. Comments on "Analytical modelling of fringe and core biodegradation in groundwater plumes". by Gutierrez-Neri et al. in J. Contam. Hydrol. 107: 1–9. J. Contam. Hydrol. 117, 1–6.
Käss, W., Schwille, F., 1992. Die "lebensdauer" von mineralöl-kontaminationen in porösen medien — erkenntnisse aus Feldbeobachrungen. In: Kreysa, G., Wiesner, J. (Eds.), Bewertung und Sanierung mineralöl-kontaminierter Böden. DECHEMA, Deutsche Gesellschaft für Chemisches Apparatewesen, Chemische Technik und Biotechnologie e.V., Frankfurt am Main, Resümee und Beiträge des 10. DECHEMA-Fachgesprächs Umweltschutz, 24.-26, pp. 533–553 (Juni 1992 in Heidelberg).
King, M.W.G., Barker, J.F., 1999. Migration and natural fate of a coal tar creosote plume 1. Overview and plume development. J. Contam. Hydrol. 39, 249–279.
King, M.W.G., Barker, J.F., Devlin, J.F., Butler, B.J., 1999. Migration and natural fate of a coal tar creosote plume 2. Mass balance and biodegradation indicators. J. Contam. Hydrol. 39, 281–307.
LaBolle, E.M., Fogg, G.E., Eweis, J.B., Gravner, J., Leaist, D.G., 2008. Isotopic fractionation by diffusion in groundwater. Water Resour. Res. 44, W07405. http://dx.doi.org/10.1029/2006WR005264.
Meckenstock, R.U., Morasch, B., Griebler, C., Richnow, H.H., 2004. Stable isotope factionation analysis as a tool to monitor biodegradation in contaminated aquifers. J. Contam. Hydrol. 75, 215–255.
Molins, S., Mayer, K.U., Amos, R.T., Bekins, B.A., 2010. Vadose zone attenuation of organic compounds at a crude oil spill site — interactions between biogeochemical reactions and multicomponent gas transport. J. Contam. Hydrol. 112, 12–29.
Naudet, V., Revil, A., Rizzo, E., Bottero, J.-Y., Bégassat, P., 2004. Groundwater redox conditions and conductivity in a contaminant plume from geoelectrical investigations. Hydrol. Earth Syst. Sci. 8, 8–22.
Ponsin, V., Coulomb, B., Guelorget, Y., Maier, J., Höhener, P., 2014a. In situ biostimulation of petroleum hydrocarbon degradation by nitrate and phosphate injection using a dipole well configuration. J. Contam. Hydrol. 171, 22–31.
Ponsin, V., Mouloubou, O.R., Prudent, P., Höhener, P., 2014b. Does phosphate enhance the natural attenuation of crude oil in groundwater under defined redox conditions? J. Contam. Hydrol. 169, 4–18.
Ponsin, V., Chablais, A., Dumont, J., Radakovitch, O., Höhener, P., 2015. 222Rn as natural tracer for LNAPL recovery in a crude oil-contaminated aquifer. Groundw. Monit. Remediat. http://dx.doi.org/10.1111/gwmr.12091 (in press).
Qiu, S., Eckert, D., Cirpka, O.A., Huenniger, M., Knappett, P., Maloszewski, P., Meckenstock, R.U., Griebler, C., Elsner, M., 2013. Direct experimental evidence of non-first order degradation kinetics and sorption-induced isotopic fractionation in a mesoscale aquifer: 13C/12C analysis of a transient toluene pulse. Environ. Sci. Technol. 47, 6892–6899.
Roberts, J.A., 2004. Inhibition and enhancement of microbial surface colonization: the role of silicate composition. Chem. Geol. 212, 313–327.
Rogers, J.R., Bennett, P.C., 2004. Mineral stimulation of subsurface microorganisms: release of limiting nutrients from silicates. Chem. Geol. 203, 91–108.
Roux, J.-C., 2006. (collective work, under the direction of), Aquifères et Eaux Souterraines de France 2 vol. BRGM éditions (956 pp.).
Sihota, N.J., Mayer, K.U., 2012. Characterizing vadose zone hydrocarbon biodegradation using carbon dioxide effluxes, isotopes, and reactive transport modeling. Vadose Zone J. 11 (4). http://dx.doi.org/10.2136/vzj2011.0204.
Trench, C.J., 2003. The U.S. Oil Pipeline Industry's Safety Performance. Allegro Energy Consulting (41 pp.).
Tuccillo, M.E., Cozzarelli, I.M., Herman, J.S., 1999. Iron reduction in the sediments of a hydrocarbon-contaminated aquifer. Appl. Geochem. 14, 655–667.
Van Liedekerke, M., Prokop, G., Rabl-Berger, S., Kibblewhite, M., Louwagie, G., 2014. Progress in the management of contaminated sites in Europe. Report EUR 26376 EN. European Commission, Joint Research Centre, Institute for Environment and Sustainability.
Wiedemeier, T.H., Rifai, H.S., Newell, C.J., Wilson, J.T., 1999. Natural Attenuation of Fuels and Chlorinated Solvents in the Subsurface. John Wiley & Sons Inc. (617 pp.).